Does the KdpA Subunit from the High Affinity K^+-Translocating P-Type KDP-ATPase have a Structure Similar to That of K^+ Channels?

Stewart R. Durell,* Evert P. Bakker,† and H. Robert Guy*

*Laboratory of Experimental and Computational Biology, Division of Basic Sciences, National Cancer Institute, National Institutes of Health, 9000 Rockville Pike, Bethesda, Maryland 20892-5677, USA, and †Abteilung Mikrobiologie, Universität Osnabrück, D-49069 Osnabrück, Germany

ABSTRACT Evidence is presented that the transmembrane KdpA subunit of the high affinity K^+-translocating P-type Kdp-ATPase is evolutionarily derived from the superfamily of 2TM-type K^+ channels in bacteria. This extends a previous study relating the K^+ channels to the KtrAB, Trk, Trk1,2, and HKT1 K^+ symporter superfamily of both prokaryotes and eukaryotes. Although the channels are formed by four single-MPM motif subunits, the transmembrane KdpA subunit and the transmembrane subunit of the symporter proteins are postulated to have four corresponding MPM motifs within a single sequence. Analysis of 17 KdpA sequences reveals a pattern of residue conservation similar to that of the symporters and channels, and consistent with the crystal structure of the KcsA K^+ channel. In addition, the most highly conserved residues between the families, specifically the central glycines of the P2 segments, are those previously identified as crucial for the property of K^+-selectivity that is common to each protein. This hypothesis is consistent with an experimental study of mutations that alter K^+ binding affinity of the Kdp transporter. Although most of the results of a previous study of the transmembrane topology of KdpA are consistent with the 4-MPM model, the one deviation can be explained by a plausible change in the structure due to the experimental method.

INTRODUCTION

Recently, we have provided indirect evidence that the transmembrane subunits (KtrB and TrkH) of two K^+ symporter protein families (KtrAB and Trk) from prokaryotes and two related K^+ symporter families (Trk1,2 and HKT1) from eukaryotes (fungi, wheat, and *Arabidopsis*) evolved from the superfamily of prokaryotic K^+ channel proteins that have M1-P-M2 (MPM, 2TM) transmembrane motifs (Durell et al., 1999; Durell and Guy, 1999). Although the K^+ channels are composed of four subunits, each with a single MPM motif, the symporters have four MPM motifs grouped in a single sequence (possibly resulting from gene duplication and fusion). The symporter TrkH subunits and the KtrB subunit from *Trepanoma pallidum* are distinguished by the existence of two additional transmembrane helices preceding the first MPM motif. Among the symporters, the KtrB subunit family appears to be closest to the presumed, common K^+ channel ancestor protein. This is because its four MPM motifs are most similar to each other, to those of both the TrkH and eukaryote K^+ symporter families, and to those of the K^+ channels. Quantification of these relative evolutionary distances was obtained by statistical comparison of numerical profiles calculated from multiple sequence alignments of the MPM motifs of each family (Durell et al., 1999). Additional support for homology was obtained by development of three-dimensional (3D) computer models that indicated similar patterns of sequence conservation over the transmembrane structure, and mutagenesis studies that identified residues in the putative P (pore) segments that alter transport of K^+ and Na^+ in the KtrAB and HKT1-type symporters (Rubio et al., 1995; Diatloff et al., 1998; Rubio et al., 1999; Tholema et al., 1999).

This work was greatly aided by the first crystal structure of a K^+ channel protein: i.e., the MPM-type KcsA channel from *Streptomyces lividans* (Doyle et al., 1998). This established the relative orientations of the different structural elements, and the molecular mechanisms by which they function. This also provided a means for judging previous K^+ channel models, and the methodologies used to development them. Of particular importance was obtaining the structure of the ion-selectivity-determining P segments, which was hypothesized to be similar in the K^+-selective symporter proteins. Specifically, in the KcsA channel structure, the four P segments are orientated with fourfold symmetry around the axis of the transmembrane pore. The first portion of each P segment (P1) assumes an α helix conformation, and is tilted to span the outer region of the bilayer and point directly toward a water-filled cavity in the center of the transmembrane region of the protein. In contrast, the latter portion of each P segment (P2) is in a relatively extended conformation, which returns the peptide chain to the outer surface of the membrane and forms the narrowest region of the channel. The K^+ binding sites are formed by the backbone carbonyl oxygens of the four P2 segments, which are oriented toward the axis of the pore. Other features established by the crystal structure are that the wider, intracellular half of the pore is formed by the four M2 α helices, and that the M1 α helices are located on the outer surface of the channel protein, where they are highly exposed to the alkyl chains of the lipids.

Received for publication 13 July 1999 and in final form 14 October 1999.

Address reprint requests to H. Robert Guy, Laboratory of Experimental and Computational Biology, Division of Basic Sciences, National Cancer Institute, National Institutes of Health, 9000 Rockville Pike, Bethesda, MD 20892-5677. Tel.: 301-496-2068; Fax: 301-402-4724; E-mail: guy@guy.nci.nih.gov.

0006-3495/00/01/188/12 $2.00

In this report, we extend the homology postulate to the KdpA subunit of the bacterial Kdp K^+ transport proteins. Kdp proteins are composed of at least three subunits: KdpA, which determines the ion selectivity (Buurman et al., 1995); KdpB, which is involved in hydrolysis of ATP and is homologous to many P-type (not to be confused with ion-selective P segments) transmembrane proteins (Hesse et al., 1984); and KdpC, which is closely coupled to KdpA and probably has one transmembrane segment (Gassel et al., 1998). Our hypothesis that KdpA is homologous to KtrB and TrkH is similar to a prior hypothesis that KdpA may have evolved from a K^+/H^+ antiporter that was recruited by the KdpB precursor to achieve the high affinity and specificity for K^+ (Epstein et al. 1990). Before our analysis, Jan and Jan (1994) identified two plausible MPM motifs in the KdpA subunit. We have expanded that postulate to include two additional MPM motifs. Our hypothesis is based on both theoretical principles and experimental evidence. First, using a KdpA sequence as the initial target, the PsiBlast procedure (Altschul et al., 1997) identifies the KtrB and TrkH subunits as the most closely related families in the database, and aligns portions of the KdpA subunit with all of the four putative MPM motifs of these symporters. This is supported by statistical comparisons of the numerical profiles of the multiply aligned sequences from each family, which indicate that the putative KdpA MPM segments are significantly more similar to those of the KtrB and TrkH subunits than they are to transmembrane segments of unrelated membrane proteins. Second, the patterns of residue conservation within the KdpA protein are similar to those of the K^+ symporters and channels. On a gross level, this is seen as the functionally important, ion-selective, putative P2 segments being highly conserved, and the most lipid-exposed, putative M1 segments being poorly conserved. Correspondingly, most of the conserved and identical residues in our alignment of KdpA with KtrB and TrkH occur either within the pore-forming P segments, or at sites within M1 and M2 that are postulated to interact with the P segments. This is supported by experimental studies identifying four clusters of mutations that affect the selectivity for K^+ (Buurman et al., 1995). Three of these clusters are located fully within three of the putative P segments, and the fourth is divided between the third putative P2 segment and the N-terminal side of the adjacent M2 segment. Finally, our model of the KdpA subunit is consistent with most of the results of an experimental study of the transmembrane topology (Buurman et al., 1995). A plausible cause for the one inconsistency is discussed.

METHODS

Sequence analysis

Standard keyword and motif searches of the NCBI's Genbank and microbial databases (see NCBI BLAST: Unfinished Microbial Genomes [http://www.ncbi.nlm.nih.gov/BLAST/unfinishedgenome.html] and NCBI Psi-Blast [http://www.ncbi.nlm.nih.gov/cgi-bin/BLAST/nph-psi blast]) were used to identify the 17 prokaryote KdpA protein sequences listed in the Appendix. The sequences of the prokaryote KtrB and TrkH symporters and 2TM K^+ channels also used here are listed in the Appendix of Durell et al. (1999). The iterative PsiBlast computer program (Altschul et al., 1997) was used to search for homologous proteins to the KdpA subunits and help form the alignments. Multiple sequence alignments were further adjusted manually to emphasize the common features of the different families. Due to the variability in the loop regions, the interfamily alignments focused primarily on the three main transmembrane segments of the putative MPM motifs (i.e., M1, P, and M2), adding as few gaps as possible.

The degree of sequence similarity between the KdpA and other protein families was quantified using a statistical profile analysis approach derived from Henikoff and Henikoff (1996) and Pietrokovski (1996). This was the same method used to study the relationship between the symporter and channel sequences in a previous report (Durell et al., 1999), which should be consulted for details. In summary, the multiple sequence alignment of each segment was first transformed into a numerical, log-odds position-specific scoring matrix. The method for constructing these profiles attempts to correct for the redundancy in the nonrandomly sampled set of known sequences in the alignments, and adds imaginary pseudocounts to estimate the real distribution of residue types at each position that occurs among all the closely related sequences in nature. Profile pairs were then compared by calculating the Pearson's correlation coefficient between each two aligned columns of residue frequencies, and then summing these up to obtain the total raw score. These scores are based on both similarities and identities of aligned residues. Raw scores were then transformed to Z scores, which are the number of standard deviations from the mean of a distribution of best chance raw scores calculated from a database of unrelated protein families. Note that, because the magnitude of the raw score depends on the length of the segment, it is necessary to calculate the Z score from a subdistribution of best chance raw scores of corresponding length. For comparisons among KdpA, the KtrB/TrkH symporters, and the 2TM K^+ channels, the global alignments of the profiles were fixed as is shown in Figs. 1 and 2 of Durell et al. (1999). In these cases, the reported Z scores are the most positive obtained for an enumeration of every possible subsegment of at least four contiguous residues. To calculate the baseline of similarity with an unrelated membrane protein family, comparisons were also made with profiles of the seven transmembrane helices of the bacteriorhodopsin family (19 sequences). In these cases, Z values of all possible alignments with no insertions or deletions were calculated for each helix. The mean of the most positive Z values from the seven helices was then used for the baseline.

RESULTS AND DISCUSSION

Sequence alignment

Figure 1 shows an alignment of the consensus sequence of the KdpA family (see Appendix) with that of the KtrB symporter family (see Durell et al., 1999) over the four putative MPM motifs. The KtrB family is used here as the reference because, as described above, it was deemed the most similar to the proposed common ancestor of its symporter superfamily (Durell et al., 1999; Durell and Guy, 1999). The alignments of the P and M2 segments were predicted primarily by the PsiBlast program (Altschul et al., 1997). This program produced ambiguous alignments for the M1 segments, e.g., the alignments were different when we began with a KtrB sequence than when we began with a KdpA sequence. These less well conserved M1 segments were manually aligned by first identifying the most hydro-

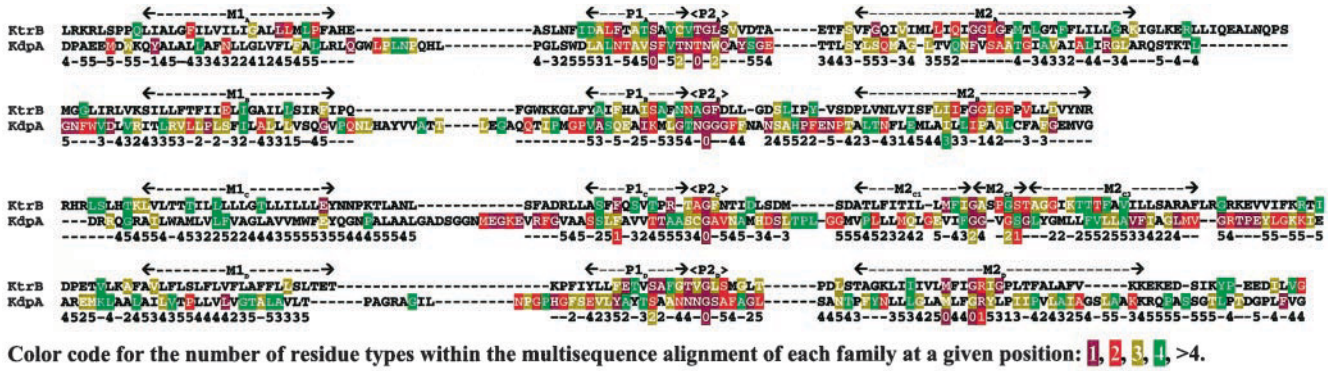

FIGURE 1 Alignment of consensus sequences of the four putative MPM motifs of the KtrB and KdpA families. Colored residues are well conserved, with the number of different types indicated by: magenta = 1, red = 2, yellow = 3, and green = 4. The numbers below the sequences indicate, for each position, the number of the three most frequently occurring residues of the KtrB plus TrkH family alignments that are not the same as any of the three most frequently occurring residues in the KdpA alignment. A dash indicates that none of the symporter residues was identical to any of the KdpA residues. The colored numbers indicate highly conserved residues (three or fewer residue types) that have identical consensus residues in all three families. See Appendix of Durell et al. (1999) for the source of KtrB and TrkH sequences and alignments.

phobic region at each location long enough to span the transmembrane region as an α helix, and then matching the more highly conserved and hydrophilic residues. The validity of our basic hypothesis is not dependent upon aligning the M1 segments correctly. The degree of conservation within each family of sequences is shown by the colored backgrounds, which indicate the number of different residues at that location: magenta = 1, red = 2, yellow = 3, green = 4, and white = 5 and greater. Although the KtrB and KdpA consensus sequences show relatively few identities, most positions have some residues that are common between the two families. As an indication, the number of the three most frequent residues of the KtrB and the TrkH families that are not among the three most frequent residues of the KdpA family are provided below the consensus sequences. Thus, larger numbers indicate less similarity between the sequence families. A dash (-) indicates that none of the residues in the KtrB and TrkH sequences are the same as the KdpA residues. In Fig. 1, the pure magenta columns with underlying zeros indicate that there are only three positions that are absolutely conserved between all the KtrB, TrkH, and KdpA sequences. Interestingly, these are the central glycines in the P2 segments of motifs B through D ($P2_{B,C,D}$). The importance of these P2 glycines in K^+ channels is indicated by the finding that their backbone carbonyl oxygens form part of the ion-binding site in the crystal structure of the KcsA channel (Doyle et al., 1998). In addition, the analogous residue is the only absolutely conserved residue among all K^+ channel subunits (Durell et al., 1999), and mutagenesis studies of the *Shaker* channel subunit indicate that it is the only residue in the P segment that cannot be mutated to cysteine without loss of K^+ selectivity (Lü and Miller, 1995). Although this glycine is not conserved in the first putative P segment of the KdpA sequences, there are four other residues in this region that are also highly conserved with the symporters. The most highly conserved of these is a serine near the C-terminal end of the $P1_A$. The importance of this serine is suggested by the fact that, when modeled after the KcsA crystal structure, this is the $P1_A$ residue closest to the pore, and thus, it likely interacts with the central residues of the P2 segment forming the ion-binding sites. It should also be noted that a serine at the analogous position in the $P1_D$ segment is also highly conserved in the KdpA and symporter sequences.

Other sites of conservation between the KdpA and symporter families occur at the central regions of the four putative M2 segments. This is especially true for the $M2_C$ and $M2_D$ segments, which have conserved unique features beyond what would be expected for a generic transmembrane helix, thus supporting the common-ancestor hypothesis. In the $M2_D$ segment, this is the central MXXGR motif, of which the glycine is the only non-P2 residue that is absolutely conserved among all symporters, and the arginine is the most highly conserved charged residue among all of the symporters.

$M2_C$ was the most difficult segment to align and model. The model that we tentatively favor is described below, but an alternative possibility is illustrated in the lower portion of Fig. 4. Previously, we have divided $M2_C$ of the symporters into three segments (Durell and Guy, 1999). The middle section ($M2_{C2}$) is rich in residues that occur frequently in random coil structures (i.e., G, S,T, P). In 3D models of the KtrB and TrkH symporters, we postulated that a coiled $M2_{C2}$ segment extends into the pore on the intracellular side of the P segments (see Figs. 2 and 4). In those models, the $M2_{C3}$ segment was postulated to be a helix that either continues the transmembrane direction of the $M2_{C1}$ segments or interact with lipids on the cytoplasmic surface of the membrane. In the KdpA sequences, however, the region with low helical propensity, $M2_{C2}$, is shorter than in KtrB

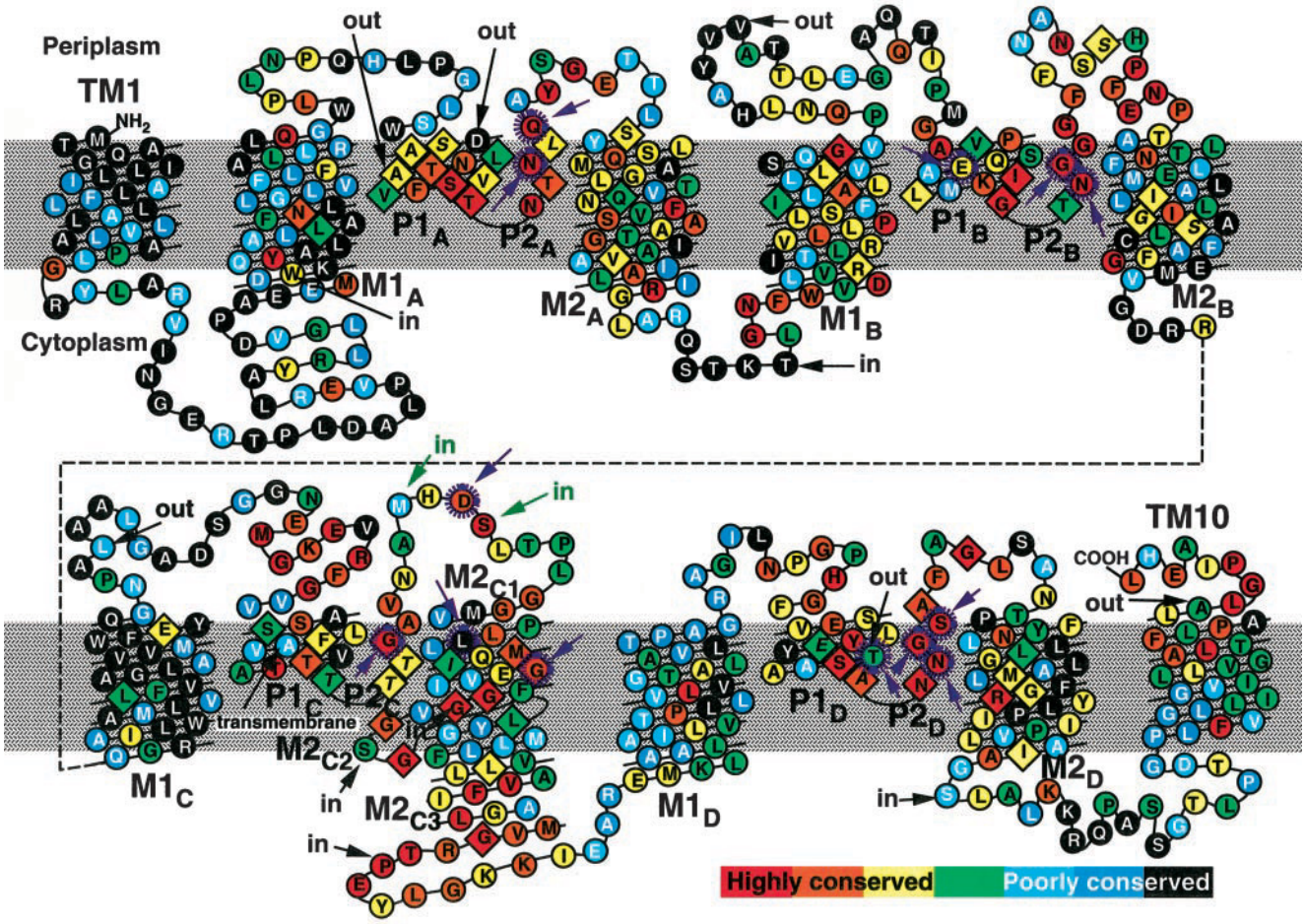

FIGURE 2 Helical net representation of the proposed transmembrane topology of KdpA. The consensus sequence is given in single-letter code. Residues are colored according to the number of residue types at each location in the alignment of 17 KdpA sequences: red = 1, orange = 2, yellow = 3, green = 4, cyan = 5, blue = 6, and black ≥7. Diamonds indicate residues that are well conserved (4 or fewer types) among the KdpA sequences, and identical to the most common or second most common residue in the KtrB and/or TrkH families. Residues encircled by purple dashes and pointed-to by purple arrows indicate positions in which mutations reduce K^+ binding (Buurman et al., 1995). The arrows labeled "out" or "in" indicate positions that fusion experiments predict are in the periplasm or cytoplasm, respectively; and a site in $P1_C$ labeled "transmembrane" had low activity for both enzymes and thus was proposed to be in the transmembrane region (Buurman et al., 1995). The green arrows indicate predictions of the fusion experiments that are inconsistent with the model presented here.

and TrkH, and the hydrophobic $M2_{C3}$ segment is longer and more highly conserved than in any of the symporters. It is interesting to note that the Trk1,2 symporters from fungi lack analogous $M2_{C2}$ and $M2_{C3}$ segments, even though they are overall evolutionarily closer to the KtrB and TrkH symporters than are the KdpA transporters (Durell et al., 1999; Durell and Guy, 1999). Three alignments of the KdpA and KtrB sequences are plausible: 1) the alignment shown in Fig. 1 aligns the most highly conserved glycines and is best for orienting the highly conserved face of the helix toward the pore as illustrated in Fig. 3 *A*, 2) an alignment in which the KdpA sequence is shifted four residues to the right is better for the $M2_{C1}$ and $M2_{C2}$ segments, and 3) an alignment in which the KdpA sequence is shifted three residues to the left is better for the $M2_{C3}$ segment.

Helical net model

Figure 2 displays a helical net model of the transmembrane topology of KdpA based on our previous models of the KtrB and TrkH symporters (Durell et al., 1999; Durell and Guy, 1999) and the sequence alignment given in Fig. 1. As seen, the major sequence of four MPM motifs is preceded and followed by single transmembrane helices, called TM1 and TM10, respectively. The single-letter amino acid codes spell out the consensus sequence of the 17 KdpA sequences (see Appendix), and their backgrounds are color-coded to indicate the number of residue types at each aligned position: red = 1, orange = 2, yellow = 3, green = 4, cyan = 5, blue = 6, and black ≥7. Diamond shaped backgrounds indicate residues that are well conserved, with four or fewer residue types, and that are also the same as the first or

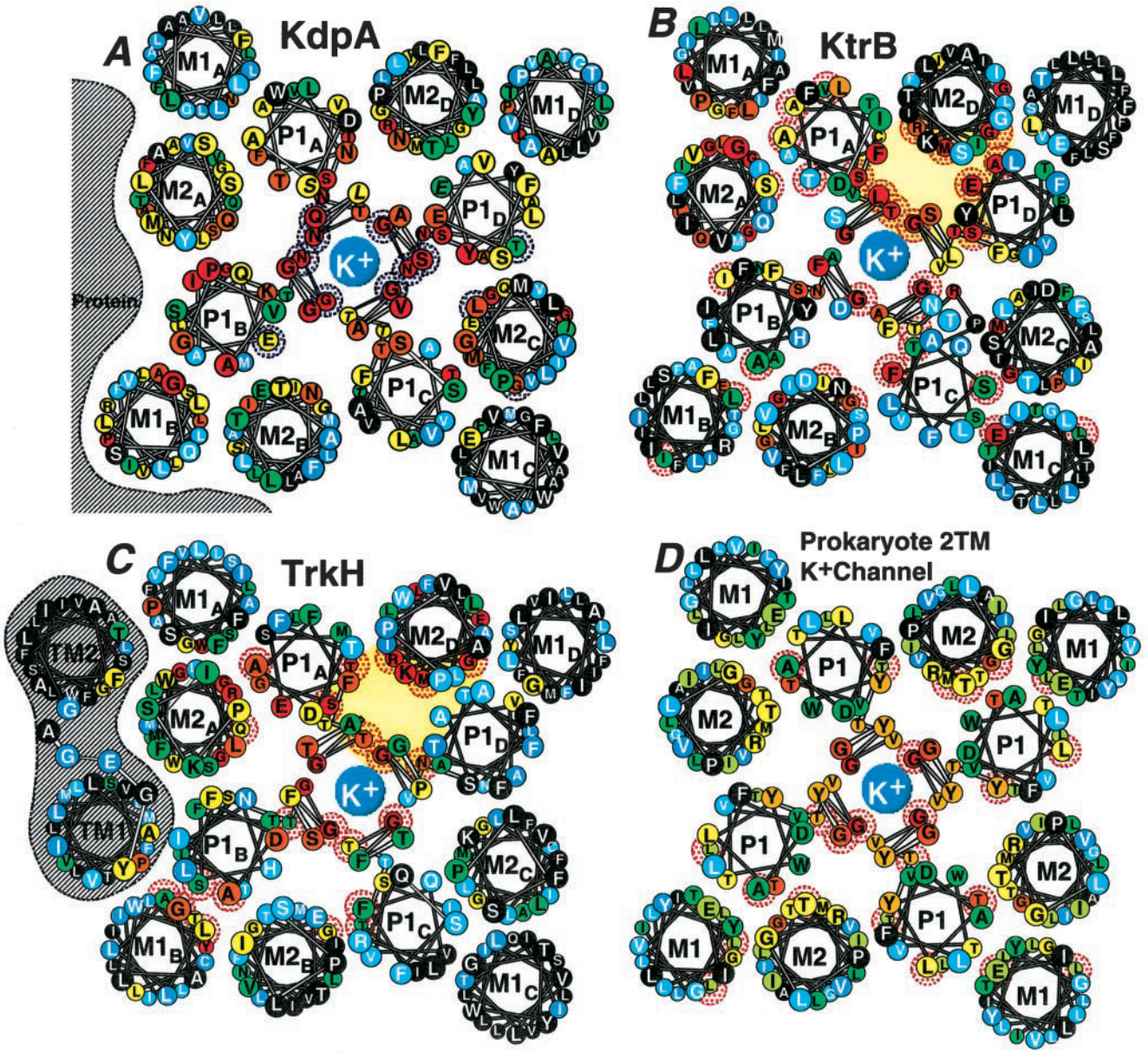

FIGURE 3 Helical wheel representation of transporters and channels viewed from outside the cell. The wheels are α helices viewed down their axes, with the small circles indicating the locations of the sidechains. The consensus sequences of the proteins are indicated by the single-letter code. The connecting loops and more cytoplasmic segments are not shown for clarity. (A) Model of KdpA: the residues surrounded by purple dots indicate positions where mutations reduce K^+ binding (Buurman et al., 1995). In the models of (*B*) KtrB, (*C*) TrkH, and (*D*) 2TM K^+ channels, the surrounding red dots indicate conserved residues within each family that are identical to conserved residues within the KdpA family. The yellow background in *B* and *C* indicates a region that is highly conserved both within and among the KdpA, KtrB, and TrkH families. For KdpA, KtrB, and TrkH, the sequences are colored according the degree of conservation as described in Fig. 2. However, a different code is used for the bacterial 2TM K^+ channels to compensate for the greater number of sequences in the alignment and the fact that they are less well conserved. In particular, residues occurring only once in the channel sequences are scored as 0.5 instead of as 1.0 to reduce the impact of a sequencing error. Thus, the color code for the channels is: red = 1–1.5; redish-orange = 2–2.5; yellowish-orange = 3–3.5; yellow = 4–4.5; yellowish-green = 5–5.5; green = 6–6.5; cyan = 7–7.5; blue = 8–8.5; black > 8.5. See Appendix of Durell et al. (1999) for the source of KtrB, TrkH, and K^+ channel sequences.

second most common residue in the KtrB and/or TrkH families (Durell et al., 1999; Durell and Guy, 1999). Note that many of these diamonds cluster at the postulated P segments forming the ion-selective region of the pore, as would be expected from the discussion of the sequence alignment (Fig. 1). Residues indicated by purple dashes and arrows indicate positions at which mutations reduced binding of K^+ (Buurman et al., 1995) (see discussion below).

In most respects, the topology in Fig. 2 is consistent with that proposed by Buurman et al. (1995) based on their

experimental results. In those studies, protein chimeras were expressed in the inner bacterial membrane with either alkaline phosphatase or β-galactosidase fused to N-terminal sequences of *Escherichia coli* KdpA of different sizes. Because the phosphatase is activated in the periplasm and the β-galactosidase is activated in the cytoplasm, it was then possible to determine the side of the membrane at which the attached enzyme was located. The results of these experiments are shown in Fig. 2 by arrows pointing to the site of attachment, and labeled "out" or "in" for periplasm or cytoplasm, respectively. The only discrepancy between the two proposed topologies is indicated by the green arrows at positions 350 and 353 in the *E. coli* KdpA sequence, which Buurman et al. (1995) found to be in the cytoplasm rather than forming a linker between the putative $P2_C$ and $M2_{C1}$ segments in the periplasm. If, as suggested in the lower portion of Fig. 4, $M2_{C3}$ forms most of the transmembrane segment with $M2_{C2}$ near the outer surface, then two more sites in $M2_{C2}$ would be inconsistent with the fusion experiments.

There are three reasons, however, to suspect that the experimental prediction for the topology at this location may be incorrect. First, examination of the KcsA crystal structure indicates that the backbone carbonyl oxygens of the C-terminal of the P1 helix and the entire P2 segment do not form hydrogen bonds with other protein atoms (consistent with their role in forming the K^+ binding site). Thus, the ability of these portions of the P segments to adopt native conformations in the outer portion of the transmembrane region is almost certainly dependent upon their being shielded from the hydrophobic lipid phase of the membrane by the surrounding M1 and M2 segments. Additionally, this P_C segment is slightly more hydrophobic than are most P segments of K^+ channels and their homologs (personal observation), and is the most hydrophobic of the putative P segments of KdpA. Thus, if insertion of the enzyme at the end of $P2_C$ and deletion of the remaining portion of the KdpA protein leaves the hydrophobic $P2_C$ segment exposed to the lipid alkyl chains, then P_C will likely adopt a transmembrane helical conformation so that the polar backbone atoms may form hydrogen bonds. This would place residues at the C-terminal of P_C (and possibly the $M2_{C2}$ segment if the $M2_{C1}$ segment is actually part of a loop region) on the cytoplasmic side of the membrane, consistent with the experimental result. Second, if the topology proposed by Buurman et al. (1995) were indeed the native topology, then the very hydrophobic putative $M2_C$ segment of our model would form part of a cytoplasmic loop rather than span the membrane. Although $M2_C$ is the most ambiguous segment in our model, it seems unlikely that a 20-residue-long segment as hydrophobic as $M2_{C3}$ does not span the membrane. The consensus sequence of $M2_{C3}$ contains no hydrophilic residues and only three ambivalent residues (three glycines). (Ambivalent means that the residue type has an almost equal probability of being buried or exposed in a soluble protein.) The segment preceding $M2_{C3}$ is also relatively hydrophobic, of the nine residues preceding $M2_{C3}$, four are hydrophobic and five are ambivalent (four glycines and a serine) and none is hydrophilic. Finally, the topology proposed by Buurman et al. (1995) places in the cytoplasm a number of residues where mutations alter the dependency of K^+ transport upon external K^+ concentration (see $P2_C$–$M2_{C1}$ residues highlighted in purple in Fig. 2). This possibility seems unlikely to us because, if cytoplasmic residues did form a second K^+ binding site as they suggest, then mutations of these residues would more likely alter the dependency of K^+ binding on the internal than on the external K^+ concentration. A more likely explanation is that these residues are located nearer the outer surface and/or outwardly accessible portion of a transmembrane pore where they are accessible to the external solution.

Helical wheel models

The postulate that the KdpA sequences are related to K^+ symporters and channels is supported by the existence of similar patterns of residue conservation over the proposed 3D structure. This is illustrated in Fig. 3 *D* by helical wheel models of the transmembrane subunits based on the KcsA channel crystal structure (Doyle et al., 1998). The wheels represent α helices viewed down their axes from the outer side of the membrane. The consensus sequences are given as single-letter codes, and the backgrounds are color-coded to indicate the degree of conservation within each family. For the KdpA, KtrB, and TrkH families, the color code is the same as in Fig. 2. A slightly different code was used for the bacterial 2TM K^+ channel family to compensate for the greater number of sequences in the alignment and the lower degree of conservation among the channel sequences (see the figure legend for details). In the KdpA model, the purple dots indicate positions where mutations were found to reduce the binding of K^+ (Buurman et al., 1995) (see discussion below). Whereas, in the KtrB, TrkH, and bacterial 2TM K^+ channel models, the red dots indicate conserved residues within each family that are the same as conserved residues within the KdpA family. It should be noted that the linkers on both the inner and outer sides of the membrane have been omitted for clarity. Additionally, the wheels only indicate the approximate relative locations of the transmembrane helices, and do not take into account the degree of tilt with respect to the axes of the pore that occurs in the KcsA crystal structure.

Overall, it is seen that the KdpA family is conserved better than are the KtrB and TrkH families, which in turn are conserved better than are the bacterial 2TM K^+ channels. For example, the aligned KdpA family of sequences has 61 absolutely conserved residues, whereas, the bacterial 2TM K^+ channel family has only one per subunit (Durell et al., 1999). The low value for the latter is unlikely due to the greater number of sequences in the alignment (27 versus 17), because the subset of the ten most closely related K^+ channel sequences still has only two absolutely conserved residues in the transmembrane region. Possible reasons for the greater degree of conservation among the KdpA se-

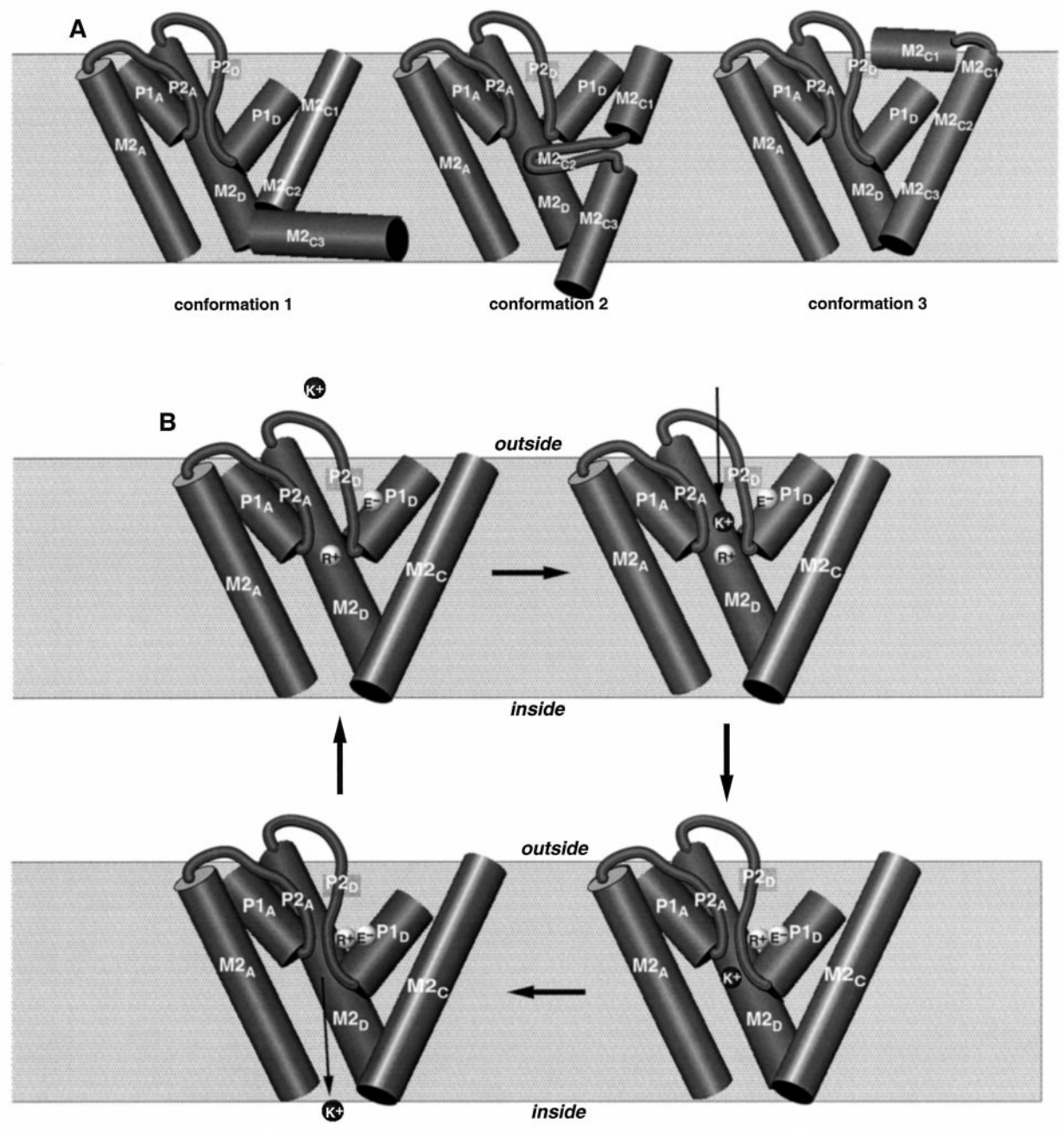

FIGURE 4 Schematic representation of plausible conformational changes in the KdpA and symporter superfamilies. The cylinders represent α helices. The view is of the side as seen from inside the pore. (*A*) Alternative conformations of the $M2_C$ segment. (*B*) An alternating access K^+ transport model. In the upper conformation, K^+ (*black sphere*) binds from the outside, but is prevented from passing through the pore by the positively charged arginine (*white sphere* labeled R^+) of $M2_D$. In the lower conformation, P_D has moved inward and/or the $M2_D$ arginine has moved outward, so that the negatively charged residue (*white sphere* labeled E^-) of $P1_D$ balances the positive charge of the $M2_D$ arginine in some of the transporters and symporters. This movement may occlude the outer pore formed by the P segments while transporting the K^+ ion to the inner cavity region, from which it dissociates into the cytoplasm. See text for details.

quences include: 1) that they are derived from a more recent common ancestor, 2) that there may be enhanced selection pressures associated with the extremely high affinity of the Kdp-ATPase for K^+ (Walderhaug et al., 1987, Hafer et al., 1989), and 3) that the functional mechanism of the ATP-dependent transport process (involving additional transmembrane subunits) is likely to be more complex.

Despite these differences in degree, each family displays similar patterns of sequence conservation, which are best seen in the schematic of the K^+ channels (Fig. 3 *D*). Spe-

cifically, the most highly conserved parts of each family are the P2 segments, which perform the K^+-selectivity function common to all. Next, it is seen that moving away from the central pore and toward the membrane-exposed periphery is associated with a decrease in sequence conservation. For example, the M1 and M2 helices of the K^+ channels clearly exhibit the pattern of unilateral conservation: where the more highly conserved polar faces are oriented toward the pore, and the poorly conserved hydrophobic faces are in contact with the alkyl chains of the membrane. Of the two, the M1 helices are the more lipid-exposed and least well conserved.

As described previously for the symporters (Durell and Guy, 1999), many of the additional highly conserved residues found in the P1 and M2 segments (compared to the channels) are likely responsible for the functional mechanisms unique to those proteins. Similarly, some of the other differentially conserved locations, especially around the perimeter, may interact with other transmembrane segments of the proteins. For example, the conserved, outwardly-oriented sides of the TrkH $M2_A$ and P_B segments were postulated to interact with the two additional transmembrane helices (shaded TM1 and TM2 region in Fig. 3 *C*) at the N-terminal of this family's sequence (Durell et al., 1999). Similarly, because the exterior faces of the putative $M1_B$, $P1_B$, and $M2_A$ segments of the KdpA family are conserved relatively well, it is predicted that they interact with the additional transmembrane helices (TM1 and TM10 in Fig. 2) and/or with the transmembrane segments of the KdpB and KdpC subunits (indicated by the shaded region in Fig. 3 *A*). The lack of these specific interactions in the channels and symporters would explain why the MPM_A and MPM_B motifs of KdpA are significantly more dissimilar from those of the other protein families than are its MPM_C and MPM_D motifs.

Statistical profile analysis

A quantitative comparison between the KdpA, KtrB/TrkH symporter, and bacterial 2TM K^+ channel families is given in Table 1. Rather than using 1-dimensional consensus sequences, the comparisons are made between sequence profiles calculated from the multiple sequence alignments of each family (see Methods). Major advantages of the profiles are that they include information about the degree of sequence conservation and the distribution of residue types at each position. The degree of similarity between each motif segment pair is given as a Z score statistic, which is the number of standard deviations that the sum of calculated correlation coefficients of the paired profile columns is from a distribution of best scores obtained by chance among unrelated protein families. Thus, the more positive the Z score, the less likely it is that the calculated correlation would occur by chance, and the more likely it is that the two families are evolutionarily related. A more detailed analysis between the symporters and channels using the same method can be found in (Durell et al., 1999).

TABLE 1 Statistical Analysis of Sequence Similarities Between Families

Segments	KdpA vs. KtrB/TrkH	KdpA vs. K^+ Channels	KtrB/TrkH vs. K^+ Channels	KdpA vs. Bacteriorhodopsin
$M1_A$	5.2	4.5	6.8	4.2
$M1_B$	4.6	3.5	6.4	3.5
$M1_C$	6.8	5.9	7.7	4.4
$M1_D$	5.3	5.1	8.2	3.8
P_A	3.0	2.2	6.3	1.8
P_B	2.6	0.7	5.1	0.9
P_C	4.2	2.0	6.3	2.1
P_D	5.2	0.9	6.1	1.9
$M2_A$	2.6	1.9	4.9	3.1
$M2_B$	4.0	3.7	5.8	3.1
$M2_C$	6.2	−0.9	6.0	3.4
$M2_D$	7.8	4.7	7.1	3.2

The first column in Table 1 presents the calculated similarities of each corresponding M1, P, and M2 segment of the four MPM motifs between the KdpA and combined KtrB/TrkH families. For interpreting these results in terms of evolutionary distance, however, it is important to control for the baseline of sequence similarity that any two unrelated transmembrane segments would have, given the preponderance of nonpolar residues in both. This is supplied by the last column in Table 1, which is the average of seven Z values obtained by aligning each KdpA segment in the optimal manner (the alignment that produces the highest Z score) with each of the seven transmembrane helices of the obviously unrelated bacteriorhodopsin membrane protein family (19 sequence homologs). The fact that all but one of the 12 Z scores is greater for the KdpA versus KtrB/TrkH comparison ($M2_A$ being the only exception) supports the contention of homology between these families. As was noted above, the similarity between the KdpA and symporter families is greater for the MPM_C and MPM_D motifs than for the other two (especially for the P and M2 segments).

To further analyze the evolutionary relationships, Table 1 also provides the separate comparisons of the KdpA and KtrB/TrkH families with the bacterial 2TM K^+ channels. From column 2, it is seen that the KdpA and channel families are significantly more distant, with only half the Z scores greater than with the bacteriorhodopsin controls. From column 3, however, it is seen that the KtrB/TrkH and channel families are considerably more similar than are the KdpA and KtrB/TrkH families, with greater Z scores for all but the $M2_C$ and $M2_D$ segments. Comparison with the bacteriorhodopsin controls (column 4) shows that, alone, the scores in column 2 do not make a compelling case for homology between the KdpA and 2TM K^+ channel families. However, the relationship is indirectly established by

the statistical calculations that both are significantly similar to the combined KtrB/TrkH family (columns 1 and 3). Because the KdpA family is calculated to be more similar to the symporter than channel families, it is likely that these two active transporter families developed from a common ancestor that previously evolved from the channels. In this case, the transition from the channel superfamily to the common ancestor would encompass the gene duplication and fusion events responsible for the single, 4-MPM motif-containing, transmembrane subunit of these proteins. This scheme is consistent with the scores produced by the Psi-Blast program, which are based on the global alignment of the entire protein sequences rather on the type of local alignments of relatively short segments used to obtain the scores in Table 1. It also is supported by the above-described findings of unique sequence features conserved in the MPM_C and MPM_D motifs of the KdpA and KtrB/TrkH families that do not occur in the single MPM motif of the 2TM K^+ channel subunits. The most prominent of these are the MXXGR motif in the $M2_D$ segments, and the cluster of helix-breaking residues in the center of the $M2_C$ ($M2_{C2}$) segments. The finding that the KdpA family is less similar to the KtrB/TrkH family than these symporters are to the channels for local alignments of the M1, P, and M2 segments indicates that the KdpA family has diverged more from the common, 4-MPM ancestor. A similar situation was observed among members of the symporter superfamily described in Durell et al. (1999). Specifically, for many segments of the prokaryote TrkH and eukaryote Trk1,2 families, the calculated similarity was no greater than that calculated here for the KdpA and KtrB/TrkH families (column 1). However, the conclusion that the TrkH and Trk1,2 families evolved from a common KtrB-like ancestor was based on the much higher scores that each of these families has with the KtrB family (Durell et al., 1999).

Correlation with mutagenesis

The most compelling data for the proposed 4-MPM motif topology and structure come from studies in which Buurman et al. (1995) screened for mutations that reduce K^+ binding of the Kdp transport system without eliminating transport. Most of the substitutions that they identified occur in the KdpA subunit, confirming this component as the major determinant of ion selectivity. This subset of 13 KdpA residues is found divided among four clusters within the sequence. Significantly, these four clusters are mostly contained within the four proposed P segments (see purple dashes and arrows in Fig. 2 and purple dots in Fig. 3 *A*). The only exception is the third cluster, which is divided between the proposed $P2_C$ segment and the N-terminal of the adjacent $M2_C$ segment. Overall, 8 of these 13 KdpA residues occur specifically in the four P2 segments, which, in analogy to the KcsA K^+ channel crystal structure (Doyle et al., 1998), form the narrowest region of the pore and the K^+ binding sites. As also seen, the remaining five residues are located directly adjacent to the pore in the KdpA model (note that the implicated D residue in the linker between $P2_C$ and $M2_C$ is not explicitly shown in Fig. 3), which could explain their experimentally determined effects on K^+ binding. For example, the glutamic acid in $P1_B$ and the aspartic acid in the linker between $P2_C$ and $M2_C$ likely act to enhance K^+ binding by making the region around the pore more electrostatically negative, whereas the threonine at the C-terminal of $P1_D$ and the leucine and glycine in $M2_C$, which, in the KdpA model of Fig. 3 *A*, face the center of the pore, likely exert steric effects.

Perhaps the most important functional link in the sequences of the KdpA, KtrB-type symporter and 2TM K^+ channel families are the central glycine residues conserved in the P2 segments. Analysis of the 2TM-type KcsA K^+ channel crystal structure (Doyle et al., 1998) shows that, not only are these glycines at the center of the narrowest pore region, but that the evolutionary invariance reflects their unique lack of a bulky, conformationally restrictive side chain. Specifically, they can easily assume a backbone conformation seldom observed for other residue types, which enables the carbonyl oxygen atoms of the P2 segments to form a linear series of closely spaced K^+ binding sites. As seen in Fig. 3 *D*, the importance of this central P2 glycine is reflected in the fact that it is the only residue identical among all the prokaryote 2TM K^+ channel sequences (indicated by red backgrounds). Similarly, of the sole four residues identical among all of the KtrB-like symporter sequences, three are the central glycines in the $P2_B$, $P2_C$, and $P2_D$ segments (Durell et al., 1999). Likewise, the analogous position in the $P2_A$ segment is a glycine in all the symporter sequences except for that of *Arabidopsis* HKT1, which has a serine substitution. For the proposed alignment of KdpA sequences presented here, glycines are also found uniquely conserved in the central regions of the latter three P2 segments. Although the analogous position in the $P2_A$ segment is an asparagine, this residue is also identical among all the KdpA sequences. In addition, these four residues all belong to the group of 13 identified as influencing K^+ binding, with the substitutions of the central glycines in the $P2_B$ and $P2_D$ segments having the largest effects of all (Buurman et al., 1995).

CONCLUSIONS

The analysis presented here and in prior publications (Durell et al., 1999; Durell and Guy, 1999) provides evidence that the K^+-selective Kdp ATPase and KtrAB/Trk families of active transport proteins evolved in prokaryotes from the superfamily of passive K^+ channel proteins. Specifically, that the more recent and functionally complex transporters have at their core the same structural molecular apparatus for providing the pore and selectivity for K^+ across the

membrane. In the transition from channels to transporters, however, this transmembrane structure has changed from a complex of four single-MPM motif subunits arranged in fourfold symmetry, to a single subunit with four MPM motifs arranged in the same configuration. At a finer level, divergences in the form of different residue identities and degrees of conservation are evident, likely reflecting the unique requirements of the different proteins.

It must be appreciated that the models of KdpA presented here are really only hypotheses based on sequence analysis and limited, indirect experimental data. Their main utility is in illustration of the homology concept and as a framework for the design of new experiments to better determine the structure and functional mechanisms. A crucial test is to determine whether the putative $P2_C$ to $M2_C$ linker of our model is in the periplasm, as we predict, or is in the cytoplasm, as proposed by Buurman et al. (1995). A related issue is whether the entire $M2_C$ segment is in the cytoplasm as proposed by Buurman et al., spans the membrane once as we propose, or twice as suggested by its length and hydropothy profile. We favor the hypothesis that $M2_C$ spans the membrane only once because it is the only possibility that is consistent with the two principle hypotheses presented here: 1) that these proteins have a K^+ ion binding region analogous to those of K^+ channels, that are formed by four P segments that, in the transporters, are related by pseudo fourfold symmetry about the axis of the pore, and 2) that KdpA is homologous to the K^+ symporters and has the same general folding pattern. (The analogous $M2_C$ segment in most of the symporters, especially Trk1,2, is too short to span the membrane twice as two α helices. Because MPM_D is the most highly conserved motif when the KdpA transporter sequences are compared to those of the symporters [see Fig. 3 and Table 1], it probably has the same orientation in the membrane in both families. This would not occur if $M2_C$ spans the membrane twice in KdpA but only once in the symporters.)

Figure 4 *A* illustrates three possible conformations for $M2_C$. In conformation 2, $M2_{C2}$ forms a loop structure that extends into the cavity region just interior to the P segments, and the $M2_{C1}$ and $M2_{C3}$ join end-to-end to form a transmembrane helix. The model helps explain why $M2_C$ is so long and why it has a central region, $M2_{C2}$, that is relatively apolar but that has a low propensity for an α helical conformation. This type of conformation would likely impede the movement of ions through the protein. Previously (Durell and Guy, 1999) we suggested that $M2_C$ of the bacterial symporters may act as part of a modulation mechanism with conformation 2 being inactive. In that model, conformation 1, in which $M2_{C3}$ lies on the cytoplasmic side of the membrane, was postulated to be the active conformation. However, the KdpA sequences are more consistent with the $M2_{C1}$ segment being part of the extracellular loop and $M2_{C3}$ being part of a transmembrane helix, as conformation 3 illustrates, because $M2_{C1}$ is substantially more polar than $M2_{C3}$. Regardless of the models, the fact that the unusual nature of $M2_C$ is conserved among KdpA, KtrB, and TrkH suggests that it is functionally important, and involvement in conformational changes of transport cannot be excluded. However, the types of large conformational changes illustrated in Fig. 4 *A* would likely to too slow to be part of the transport cycle, and the fact that the eukaroyte symporters have no segment analogous to $M2_{C2}$ (Durell et al., 1999) suggests that this structure is not essential to the K^+ transport process itself.

Do these models suggest a mechanism to transport K^+ against its electrochemical gradient that is common to the KdpA transporters and the symporters but that is not present in the channels? The primary distinguishing characteristic between a channel and an alternating access model of a transporter is the presence of a barrier or barriers that prevent free diffusion of the ion through the transmembrane region of the protein (Jardetzky, 1966). An alternating access model of a K^+ transporter has two conformations, the first allows K^+ to bind from the outside but has a barrier that prevents it from diffusing to the inside, and the second allows K^+ to pass the barrier and diffuse into the cell but has a barrier that prevents it from diffusing back to the outside. The positively charged arginine of $M2_D$ is the most conserved charged residue among all the KdpA and symporter sequences; it is present in all KdpA, TrkH, and Hkt1 sequences and almost all KtrB and Trk1,2 symporters, but it is not present in any known K^+ channel sequence. (However, a subfamily of putative 2TM K^+ channel subunits found in *Streptomyces coelicolor*, *Corynebacterium diphtheriae*, *Mycobacterium tuberculosis*, and *Mycobacterium avium* do have an arginine in the analogous position.) In the model illustrated in Fig. 4 *B*, this arginine may act as at least part of an energy barrier to free diffusion of K^+ ions through the pore in both conformations. When the transporters are modeled after the KcsA structure, this arginine side chain extends into a region just interior to the P segments (Durell and Guy, 1999) that forms a large water-filled cavity in the KcsA structure, as illustrated in the upper portion of Fig. 4 *B*. In this conformation, its charge should be balanced by the negatively charged ends of the P2 helical dipoles (Roux and MacKinnon, 1999). Placed here, the arginine should not prevent K^+ ions from entering the pore from the outside and binding between the P2 segments, but it should impede the movement of a K^+ ion into the cavity region. When the protein conformation changes to that in the lower portion of Fig. 4 *B*, the K^+ ion is transported to the cavity region of the transporter from which it can dissociate to the cytoplasm and the arginine side chain moves to the extracellular side of the K^+ ion, where it presents an energy barrier to diffusion of the K^+ ion back to the outside. The conformational change could involve an inward movement P_D as illustrated here, and/or possibly an outward movement of $M2_D$, however, it could be as subtle as a conformational change of the arginine side chain alone

(see Durell and Guy, 1999 for illustrations of the latter two possibilities). It could also involve conformational changes within $M2_C$ (not illustrated). All KtrB and eukaryote K^+ symporters have a glutamate on the pore-oriented face of $P1_D$, and most KdpA sequences also have a glutamate either at the same place or nearby four residues earlier in the sequence (see Figs.1 and 2). In these proteins, the arginine's positively charged side chain may bind to the negatively charged glutamate side chain on $P1_D$. However, the negatively charged group on $P1_D$ is not essential because TrkH symporters and some KdpA proteins do not have a negatively charged residue on $P1_D$. In these cases, the arginine side chain may become deprotonated, at least during the conformational change when the K^+ ion and the arginine move past each other. This possibility is especially attractive for TrkH because these symporters use H^+ as the cotransported ion. Thus, the arginine side chain may act as a proton shuttle for Trk symporters with H^+ dissociating to the cytoplasm in the upper conformation as K^+ enters from the outside, and with another H^+ binding from the outside in the lower conformation as K^+ dissociates to the inside.

In the symporters, the energy to drive the transport cycle comes from movement of the cotransported ion, Na^+ or H^+, down its electrochemical gradient. In the Kdp system, the energy comes from the hydrolysis of ATP by the KdpB subunit (not illustrated). Coupling between the KdpA and KdpB subunits may involve the segment at the end of $M2_D$, because this region shows some homology with other transport ATPases (Buurman, et.al., 1995). It could also involve the $M2_{C3}$ segment, which is highly conserved among the KdpA sequences (see Figs. 1 and 2), but is not well conserved among the symporters. In either case, the transport process would likely involve movement of at least one of the M2 segments.

A potentially problematic aspect of our model is that, in KdpA, the first half of most of the putative M2 segments contains negatively charged and/or noncharged hydrophilic residues. The presence of these residues is, however, consistent with our hypothesis that these proteins are similar to K^+ channels. The first, and typically more highly conserved, of these hydrophilic residues is near the N-terminus and aligns with a position usually occupied by a lysine in the K^+ channels. In the KcsA structure, the side chain of this residue extends toward the pore and is exposed to the extracellular solution. For the remaining hydrophilic residues, hydrophilic and negatively charged residues are found in analogous locations in the M2 segment of inwardly rectifying K^+ channels and/or in S6 segments of some cyclic nucleotide-gated channels and plant K^+ channels (personal observation). In our models, these residues face inward where they could either interact with the channel-forming P segments, or extend into the channel interior to the P segments (see Fig. 3 *A*). With the exception of the arginine in $M2_D$, these hydrophilic residues are not absolutely conserved among the KdpA sequences, and thus are unlikely to be crucial for the transport process.

APPENDIX

TABLE A1 Sources of KdpA Sequences

Organism	Accession	Data: Base source	Accession
Alicyclobacillus acidocaldarius	CAB45636	embl:AAC243194	AJ243194.1
Clostridium acetobutylicum	O32327	Swiss:ATKA_CLOAB	O32327
Escherichia coli	P03959	Swiss:ATKA_ECOLI	P03959
Mycobacterium tuberculosis	P96371	Swiss:ATKA_MYCTU	P96371
Synechocystis PCC6803	P73866	Swiss:ATKA_SYNY3	P73866

Unfinished Genomes	gnl
Bordetella bronchiseptica	Sanger
Bordetella pertussis	Sanger|B.pertussis_Contig403:Contig628
Deinococcus radiodurans	TIGR|D.radiodurans_8807
Campylobacter jejuni	Sanger|campylo_Cj.seq
Caulobacter crescentus	TIGR|C.crescentus_gcc_631
Enterococcus faecalis	TIGR|gef_6355
Mycobacterium avium	TIGR|M.avium_5491;1363
Pseudomonas aeruginosa	PAGP|Paeruginosa_Contig53
Salmonella typhi	Sanger|S.typhiContig1782
Staphylococcus aureus	TIGR|S.aureus_gsa_272
Thiobacillus ferrooxidans	TIGR|t_ferrooxidans_570
Yersinia pestis	Sanger|Y.pesits_Contig793

The work in Osnabrück was supported by the Deutsche Forschungsgemeinschaft (SFB171) and the Fonds der Chemischen Industrie. Some preliminary sequence data were obtained from The Institute for Genomic Research website at http://www.tigr.org and the NCBI website at http://www.ncbi.nlm.nih.gov/BLAST/unfinishedgenome.html.

REFERENCES

Altschul, S. F., T. L. Madden, A. A. Schaffer, J. Zhang, Z. Zhang, W. Miller, and D. J. Lipman. 1997. Gapped BLAST and PSI-BLAST: a new generation of protein database search programs. *Nucleic Acids Res.* 25:3389–3402

Buurman, E. T., K.-T. Kim, and W. Epstein. 1995. Genetic evidence for two sequentially occupied K^+ binding sites in the Kdp transport ATPase. *J. Biol. Chem.* 270:6678–6685

Diatloff, E., R. Kumar, and D. P. Schachtman. 1998. Site directed mutagenesis reduces the Na^+ affinity of HKT1, an Na^+ energized high affinity K^+ transporter. *FEBS Lett.* 432:31–36

Doyle, D. A., J. M. Cabral, R. A. Pfuetzner, A. Kuo, J. M. Gulbis, S. L. Cohen, B. T. Chait, and R. MacKinnon. 1998. The structure of the potassium channel: molecular basis of K^+ conduction and selectivity. *Science.* 280:69–77

Durell, S. R., Y. Hao, T. Nakamura, E. P. Bakker, and H. R. Guy. 1999. Evolutionary relationship between K^+ channels and symporters. *Biophys. J.* 77:775–788.

Durell, S. R., and H. R. Guy. 1999. Structural models of the KtrB, TrkH and Trk1,2 symporters based on the structure of the KcsA K^+ channel. *Biophys. J.* 77:789–807.

Epstein, W., M. O. Walderhaug, J. W. Polarek, J. E. Hesse, E. Dorus, and J. M. Daniel. 1990. The bacterial Kdp K(+)-ATPase and its relation to other transport ATPases, such as the Na+/K(+)- and Ca2(+)-ATPases in higher organisms. *Philos. Trans. R. Soc. Lond. B. Biol. Sci.* 326: 479–487.

Gassel, M., A. Siebers, W. Epstein, and K. Altendorf. 1998. Assembly of the Kdp complex, the multi-subunit K^+-transport ATPase of *Escherichia coli*. *Biochim. Biophys. Acta.* 1415:77–84.

Hafer, J., A. Siebers, and E. P. Bakker. 1989. The high-affinity K^+-translocating ATPase complex from *Bacillus acidocaldarius* consists of three subunits. *Mol. Microbiol.* 3:487–495

Henikoff, J. G., and S. Henikoff. 1996. Using substitution probabilities to improve position-specific scoring matrices. *Comput. Appl. Biosci.* 12: 135–143

Hesse, J. E., L. Wieczorek, K. Altendorf, A. S. Reicin, E. Dorus, and W. Epstein. 1984. Sequence homology between two membrane transport ATPases, the Kdp-ATPase of *Escherichia coli* and the Ca^{2+}-ATPase of sarcoplasmic reticulum. *Proc. Natl. Acad. Sci.* USA. 81:4746–4750

Jan, L. Y., and Y. N. Jan. 1994. Potassium channels and their evolving gates. *Nature.* 371:119–122

Jardetzky, O. 1966. Simple allosteric model for membrane pumps. *Nature.* 211:969–970.

Lü, Q., and C. Miller. 1995. Silver as a probe of pore-forming residues in a potassium channel. *Science.* 268:304–307

Pietrokovski, S. 1996. Searching databases of conserved sequence regions by aligning protein multiple-alignments. *Nucleic Acids Res.* 24: 3836–3845

Roux, B., and R. MacKinnon. 1999. The cavity and pore helices in the KcsA K^+ channel: electrostatic stabilization of monovalent cations. *Science.* 285:100–102

Rubio, F., W. Gassmann, and J. I. Schroeder. 1995. Sodium-driven potassium uptake by the plant potassium transporter HKT1 and mutations conferring salt tolerance. *Science.* 270:1660–1663

Rubio, F., M. Schwarz, W. Gassmann, J. I. Schroeder. 1999. Genetic selection of mutations in the high affinity K^+ transporter HKT1 that define functions of a loop site for reduced Na^+ permeability and increased Na^+ tolerance. *J. Biol. Chem.* 274:6839–6847

Tholema, N., E. P. Bakker, A. Suzuki, and T. Nakamura. 1999. Change to alanine of one out of four selectivity filter glycines in KtrB causes a two orders of magnitude decrease in the affinities for both K^+ and Na^+ of the Na^+ dependent K^+-uptake system KtrAB from *Vibrio alginolyticus*. *FEBS Lett.* 450:217–220

Walderhaug, M. O., D. C. Dosch, and W. Epstein. 1987. Potassium transport in bacteria. *In* Ion Transport in Prokaryotes, B. P. Rosen, and S. Silver, editors. Academic Press, New York. 85–130.